IgG biofilm adsorption is influenced by Cobalt wear debris size and can increase IL-1beta production in macrophages

Reddy, A; Caicedo, M; Jacobs, JJ and +Hallab, NJ
Department of Orthopedic Surgery, Rush University Medical Center, Chicago, IL 60612
nhallab@rush.edu

INTRODUCTION: Metallic implant debris may exist *in vivo* as particles (micrometers to nanometers in size), or colloidal and ionic forms of metal (specifically or nonspecifically bound by protein). The biocompatibility of metallic implant surfaces is governed in large part by the interfacial kinetics associated with protein binding. (1) Immediately upon implantation, biomaterial surfaces complex with proteins forming a protein biofilm. The composition of adsorbed proteins and subsequent cell-material interactions are determined by the physiochemical properties of the biomaterial. (1) Because the biofilm is an intermediary between biomaterial surfaces and host tissue, it is necessary to characterize the interface in terms of the adsorbed biofilm. Previous studies showed differences in protein binding based on differences in the type of material (metal vs polymer and Ti-alloy vs Co-alloy) (1). Can these differences in protein binding exist in a specific metal of different size particles? Previous studies implicated interactions between IgG proteins and alloy surfaces as an inducer of bioreactivity. We hypothesized that a given implant alloy will show differences in protein biofilm based on particle size alone (when analyzed on an equal surface area basis) and that these biofilm difference will impact bioreactivity in vitro, where IgG biofilms will induce greater bioreactivity than other common serum proteins (Albumin). We tested this hypothesis by analyzing the biofilm of 2 sizes of Co-alloy particles in human serum and by altering the biofilm of a single size of Co-alloy particles and measuring the consequent bioreactivity.

MATERIALS AND METHODS: N=6 subjects were consented and used to obtain human serum for biofilm and bioreactivity testing. To assess biofilm differences two sizes of CoCrMo implant alloy (ASTM F75) spherical particles were used: diameters of (1-5um) ≈4.7um and ≈70um (volume basis, mv) (Bioengineering Solutions Inc.). Equal surface areas were used to assess biofilm adsorption with each size type: 100 cm^2. Particles were incubated for 4 days in serum provided by 6 subjects. Beads were gently washed with PBS 2x, to remove non-adherent proteins then biofilm proteins were eluted with 2% SDS solution for 24 hours. Samples were then separated and analyzed by 1-d SDS gel 10-20% (Bio-Rad). Coomassie blue stained gels were analyzed using NIH scion image to determine protein amounts compared to known standards (Bio-Rad). To determine the bioreactivity of biofilm differences found in the first part of this study, a comparative study examined the effects of fibronectin, serum, albumin, IgG and LPS biofilms incubated with 1 micron-sized particles dosed at 5 particles/cell on early cytokine TNF-alpha and 24-hour IL-1beta cytokine release in autologous primary human monocytes/macrophages (n=5).

RESULTS: The eluted biofilm gels of 3 subjects are shown in **Fig 1**. Data analsysis of the 140kD band is shown in **Fig. 2**. Biofilms of the specimens from all 6 subjects demonstrated compositional and total differences in amount of serum proteins adsorbed onto Co-based alloy beads. Densitometric analysis of the biofilm protein bands revealed that the only statistically significant difference in the intensity of protein(s) binding between the metals was in 140 kDa molecular weight (rectangular box present in **Fig 1**) ($p < 0.05$) (when represented as a percentage of total serum protein adsorbed). Normalization was used to account for introduced and inherent variability in total protein between subjects. There was subject-dependent variation in the total protein adsorbed onto the metal surfaces, despite identical processing of all samples possibly related to endogenous constitutive protein differences. Thus there were no significant size-dependent differences in total amounts of bound proteins, but more samples are necessary to corroborate this phenomenon. Bioreactivity of albumin and IgG biofilm differences using 1um sized Co-alloy particles were assessed using primary monocytes/macrophages and the results of TNF-α and IL-1β are shown in **Figs. 3 and 4**. Biofilm differences induced statistically significant differences in IL-1β secretion and increased significant differences in the albumin secretion of TNF-α over that of IgG (results for one of 5 individuals shown, **Fig 4**).

DISCUSSION: The results of this investigation only partially supported our original hypothesis. We did identify particle-size based dependence of serum bioflims. However when these biofilm differences were imposed on particles of the same size (1um), they did not induce bioreactivity differences. Smaller sized particles (5um) preferentially bound large range proteins especially in ≈140kD range as did larger particles (70um). Since this characteristic was consistent with all subjects it seems that other surface characteristics (e.g. surface charge density, microstuctural variation, etc.) rather than alloy composition (i.e.Co-alloy) play a role in differential binding. The lack of influence of biofilm composition on cytokine production was unexpected. In all subjects IgG biofilms did not play as significant a role in TNF-alpha production as did albumin. A mix of serum proteins which includes IgG were shown to play a more important role in eliciting an inflammatory response (inflammasome induced IL-1β, **Fig 4**). Further testing using Western blot, 2D-PAGE, and Mass Spec analyses are the focus of current efforts to more fully identify and investigate biofilm proteins on implant debris and their associated biologic effects.

ACKNOWLEDGEMENTS: NIAMS/NIH, Crown Family Chair of Orthopedics

REFERENCES: 1. Hallab NJ et al. Systemic metal-protein binding associated with total joint replacement arthroplasty. J Biomed Mater Res 2000;49:353–361.

Figure 1.

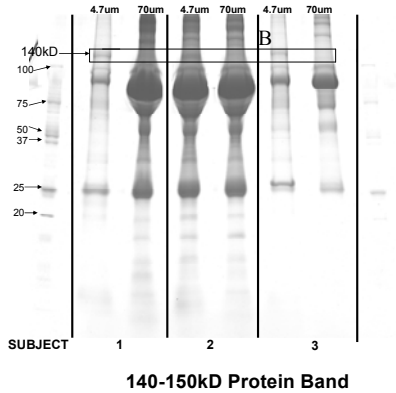

Figure 2.

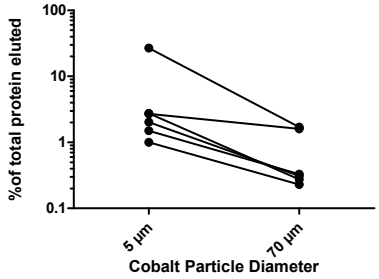

Figure 3.

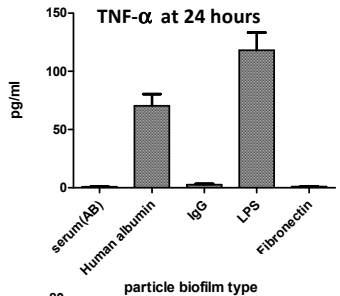

Figure 4.